Source Tracking with Multiple-Forgetting-Factor RLS Using a Vector-Hydrophone Away From or Near a Reflecting Boundary

Kainam Thomas WONG (ktwong@ieee.org)
Department of Electrical & Computer Engineering, University of Waterloo, Waterloo, Ontario, N2L 3G1, Canada

Mohamad Khattar AWAD (mohamad@ieee.org)
Department of Electrical & Computer Engineering, University of Waterloo, Waterloo, Ontario, N2L 3G1, Canada

***Abstract*— A vector-hydrophone (a.k.a. acoustic vector-sensor) is composed of two or three spatially collocated but orthogonally oriented velocity-hydrophones, possibly plus a collocated pressure-hydrophone. A vector-hydrophone may form azimuth-elevation spatial beams that are invariant with respect to the sources' frequencies, bandwidths and radial locations (i.e., in near field as opposed to the far field). This paper adopts a multiple-forgetting-factor recursive-least-squares (RLS) adaptive algorithm to a single vector-hydrophone for source tracking, without needing any prior knowledge of the source power and/or the noise powers.**

I. Introduction

A velocity-hydrophone measures one Cartesian component of the three-dimensional particle-velocity vector of the incident wavefield. Velocity-hydrophone technology has existed for decades in the field of underwater acoustics [1] and is the subject of renewed interest [7]. A four-component vector-hydrophone has two or three orthogonally oriented velocity-hydrophones and possibly a pressure hydrophone, all collocated in a point-like geometry. Vector-hydrophones are commercially available as the "Uniaxial P-U Probe" from Acoustech[1] [23]. Vector-hydrophones have undergone sea trials [2],[3],[4],[5],[13],[19]. When a four-element vector-hydrophone (located at the coordinates' origin) is placed near a reflecting boundary plane of infinite size and situated at $z = -D$, its 4×1 array manifold equals [18]:

$$\mathbf{a}(\theta,\varphi) \quad \stackrel{\text{def}}{=} \quad \left\{1 + R(\theta)e^{-j4\pi\frac{D}{\lambda}\sin\theta}\right\}\begin{bmatrix} u(\theta,\varphi) \\ v(\theta,\varphi) \\ w(\theta) \\ 1 \end{bmatrix} \\ -2R(\theta)e^{-j4\pi\frac{D}{\lambda}\sin\theta}\begin{bmatrix} 0 \\ 0 \\ w(\theta) \\ 0 \end{bmatrix} \qquad (1)$$

where $0 \le \theta_k < \pi/2$ symbolizes the elevation angle measured from the vertical x-y plane[2], $0 \le \varphi_k < 2\pi$ denotes the azimuth angle measured from the positive x-axis, $u(\theta,\varphi) = \cos\theta\cos\varphi$ refers to the diction-cosine along the x-axis, $v(\theta,\varphi) = \cos\theta\sin\varphi$ refers to the diction-cosine along the y-axis, $w(\theta) = \sin\theta$ refers to the diction-cosine along the z-axis, and λ symbolizes the source's wavelength. Three special cases exist:

1) No reflecting boundary exists near the vector-hydrophone: $R(\theta) = 0$ [6]. Thus, (1) degenerates to: [6],[23]
$$\mathbf{a}(\theta,\varphi) \stackrel{\text{def}}{=} \begin{bmatrix} \mathbf{d} \\ 1 \end{bmatrix} \stackrel{\text{def}}{=} \begin{bmatrix} \cos\theta\cos\varphi \\ \cos\theta\sin\varphi \\ \sin\theta \\ 1 \end{bmatrix} \qquad (2)$$
A four-component vector-hydrophone would thus measure all three Cartesian components of the acoustic velocity vector-field plus the overall pressure scalar-field. Direction finding [16] [21] and source tracking [20] using a single vector-hydrophone would require no a priori information of the signals' bandwidth and spectra, because the array manifold is entirely independent of signal frequency due to the spatial co-location of its constituent sensors. The complicating effects of a near-field wave-front's curvature is also avoided because of the spatial co-location of the vector-hydrophone's constituent sensors.
2) For a rigid reflecting boundary (such as a ship hull at high frequency), $R(\theta) \approx 1, \forall\theta$ [18].
3) For a pressure-releasing reflecting boundary (such as the sea-air interface or the ship hull at low frequency), $R(\theta) \approx -1, \forall\theta$ [18].

An array of *multiple* vector-hydrophones are used with maximum-likelihood estimation in [8], with ESPRIT in [10], [11], [16], [17], with MUSIC in [17], [26] and with Root-MUSIC in [15], with least-squares based algorithms in [24], with beamspace direction-finding in [12],[25].

Whereas [20] applies Kalman filtering to a three-component vector-hydrophone (without the pressure hydrophone), this present work will instead propose an adaptive RLS tracking algorithm using multiple forgetting factors [9].

II. RLS Tracking of a Single Source Using a Vector-Hydrophone

A. A Mathematical Statement of the Tracking Problem

The statistical data model is as follows: A real-valued signal, of frequency f and power σ_s^2, impinges upon a vector-hydrophone[3]

[0]This work was supported by Canada's Natural Sciences & Engineering Research Council's Individual Research Grant # NSERC-RGPIN-249775-02 and the Premier's Research Excellence Award from the province of Ontario.
The authors are grateful to Dr. Petr Tichavský for critically useful discussions.

[1]http://www.acoustechcorporation.com

[2]$|\theta_k| \le \pi/2$ if $R(\theta) = 0$.

[3]When there is a boundary, the z-axis velocity-hydrophone is not needed. For the no-boundary case, the pressure-hydrophone is not needed.

located at $(0,0,0)$. After carrier-frequency down-conversion, the vector-hydrophone's collected data equal:

$$\mathbf{z}(t) \quad = \quad \mathbf{a}(\theta(t),\varphi(t))s(t)+\mathbf{n}(t) \tag{3}$$

where $\mathbf{a}(.,.)$ is as defined in (1) or (2), except now with a time-varying $(\theta(t),\varphi(t))$. The 4×1 noise vector $\mathbf{n}(t) = [n_{v_x}(t), n_{v_y}(t), n_{v_z}(t), n_p(t)]^T$ is complex-valued, statistically uncorrelated across its components and over t, with mean $[0,0,0,0]^T$ and covariance matrices:

$$\begin{aligned} E\left[\mathbf{n}(t)\mathbf{n}^H(s)\right] &= \delta(t-s)\text{diag}\{\sigma_v^2,\sigma_v^2,\sigma_v^2,\sigma_p^2\} \\ E\left[\mathbf{n}(t)\mathbf{n}^T(s)\right] &= \text{diag}\{0,0,0,0\},\ \ \forall t,s \end{aligned}$$

where the superscript ^{T} denotes transposition, the superscript ^{H} denotes the Hermitian operation, diag{ } symbolizes a diagonal matrix having as its diagonal elements that which are inside { }. With T denoting the time-sampling period and given $\mathbf{Z} = \{\mathbf{z}(nT),\ n=0,1,2,...\}$, the present problem is to adaptively estimate $(\theta(nT),\varphi(nT))$ over n.

B. Single-Forgetting-Factor Tracking

The recursive least-squares (RLS) algorithm is adopted here for uni-vector-hydrophone tracking as follows: [6]

$$\mathbf{p}(nT) \quad = \quad \frac{\text{Re}\left\{\begin{bmatrix}[\mathbf{z}(nT)]_1\\ [\mathbf{z}(nT)]_2\end{bmatrix}\right\}}{\text{Re}\left\{[\mathbf{z}(nT)]_4\right\}} \tag{4}$$

$$\hat{\mathbf{d}}_N = \begin{bmatrix}\hat{u}_N\\ \hat{v}_N\end{bmatrix} \quad = \quad \frac{\sum_{n=0}^{N}\lambda^{-n}\,\mathbf{p}(nT)}{\sum_{n=0}^{N}\lambda^{-n}} \tag{5}$$

The above leads to the recursive relation [14]:

$$\hat{\mathbf{d}}(nT) \quad = \quad \lambda\hat{\mathbf{d}}(nT-T)+(1-\lambda)\mathbf{p}(nT) \tag{6}$$

for $n=1,2,\ldots,N$. Hence,

$$\hat{\theta}_N \quad = \quad \arccos\left(\sqrt{\hat{u}_N^2+\hat{v}_N^2}\right) \tag{7}$$

$$\hat{\varphi}_N \quad = \quad \angle\left(\hat{u}_N+j\hat{v}_N\right) \tag{8}$$

In the above, $\lambda<1$ represents a "forgetting factor", the superscript * denotes complex conjugation, and $[\mathbf{v}]_i$ denotes the ith element in the vector $\mathbf{v}$. The denominator in (4) corrects for the signal steering-vector's time-varying dependence on θ of (1) and for the signal amplitude $s(t)$ in (3). For the no-boundary special case, where $R(\theta)=0$, substitute (4) through (5) by the following three steps:

$$\mathbf{p}(nT) \quad = \quad \frac{\text{Re}\left\{\begin{bmatrix}[\mathbf{z}(nT)]_1\\ [\mathbf{z}(nT)]_2\\ [\mathbf{z}(nT)]_3\end{bmatrix}\right\}}{\left\|\text{Re}\left\{\begin{bmatrix}[\mathbf{z}(nT)]_1\\ [\mathbf{z}(nT)]_2\\ [\mathbf{z}(nT)]_3\end{bmatrix}\right\}\right\|} \tag{9}$$

$$\bar{\mathbf{d}}_N \quad = \quad \left(\sum_{n=0}^{N}\lambda^{-n}\right)^{-1}\sum_{n=0}^{N}\lambda^{-n}\,\mathbf{p}(nT) \tag{10}$$

$$\hat{\mathbf{d}}_N \quad = \quad \begin{bmatrix}\hat{u}_N\\ \hat{v}_N\\ \hat{w}_N\end{bmatrix} \quad = \quad \frac{\bar{\mathbf{d}}_N}{\|\bar{\mathbf{d}}_N\|} \tag{11}$$

The above leads to the recursive relation [14]:

$$\hat{\mathbf{d}}(nT) = \frac{\lambda\hat{\mathbf{d}}(nT-T)+(1-\lambda)\mathbf{p}(nT)}{\|\lambda\hat{\mathbf{d}}(nT-T)+(1-\lambda)\mathbf{p}(nT)\|} \tag{12}$$

for $n=1,2,\ldots,N$. The denominator in (9) corrects for the signal amplitude $s(t)$ in (3) and implicitly performs noise cancelation. An appropriate pre-set value of λ is critical to this single-forgetting-factor RLS tracking algorithm. However, λ depends, in a complicated way, on the variance σ_w^2 of the incident source's spatial motion and on the signal-to-noise ratios $\frac{\sigma_s^2}{\sigma_v^2}$ and $\frac{\sigma_s^2}{\sigma_p^2}$, which are all typically a priori unknown. In the absence of such prior information, multiple-forgetting-factor tracking [9] may be used, as it requires no pre-set value for λ but can self-tune λ.[4]

C. Multiple-Forgetting-Factor Adaptation

This approach[5] uses M different forgetting factors $\{\lambda_1,\ldots,\lambda_M\}$ (ordered in decreasing magnitude) in parallel on the same data $\{\mathbf{p}(nT), n=1,2,3\ldots N\}$, producing the M estimates $\{\hat{\mathbf{d}}^{(m)}(nT), m=1,\ldots,M\}$ of the vector $\boldsymbol{a}(nT)$. λ_1 would produce a stable but slowly converging estimate, whereas λ_M would yield a responsive but erratic estimate. These M estimates are here adaptively weighted to fit the source's time-varying movement. A weighted average of $\{\hat{\mathbf{d}}^{(m)}(nT),\ m=1,\ldots,M \text{ and } n=1,\ldots,N\}$ produces a combined estimate,

$$\hat{\mathbf{d}}(nT) = \sum_{m=1}^{M}\beta^{(m)}(n)\hat{\mathbf{d}}^{(m)}(nT) \tag{13}$$

where $\sum_{m-1}^{M}\beta^{(m)}(n)=1$; $0\le\beta^{(m)}(n)\le 1, \forall m,n$; and

$$\hat{\mathbf{d}}^{(m)}(nT) \quad = \quad \frac{\lambda_m\hat{\mathbf{d}}(nT-T)+(1-\lambda_m)\mathbf{p}(nT)}{\|\lambda_m\hat{\mathbf{d}}(nT-T)+(1-\lambda_m)\mathbf{p}(nT)\|} \tag{14}$$

for the near-boundary case of (1), and

$$\hat{\mathbf{d}}^{(m)}(nT) \quad = \quad \lambda_m\hat{\mathbf{d}}(nT-T)+(1-\lambda_m)\mathbf{p}(nT) \tag{15}$$

for the no-boundary case of (2). Moreover,

$$x^{(m)}(n) \quad = \quad \|\mathbf{p}(nT)-\hat{\mathbf{d}}^{(m)}(nT-T)\| \tag{16}$$

$$\beta^{(m)}(n) \quad = \quad \frac{\beta^{(m)}(n-W)\prod_{l=n-W+1}^{n}p(x^{(m)}(l)|m)}{\sum_{j=1}^{M}\beta^{(j)}(n-W)\prod_{l=n-W+1}^{n}p(x^{(m)}(l)|j)} \tag{17}$$

$$\beta^{(m)}(n-W) \quad = \quad \frac{1}{M} \tag{18}$$

$$p(x^{(m)}(n)|m) \quad = \quad \frac{1}{\sqrt{2\pi}\hat{\sigma}(n)}\exp\left\{-\frac{x^{(m)}(n)}{2\hat{\sigma}^2(n)}\right\} \tag{19}$$

$$\hat{\sigma}^2(n) \quad = \quad \sum_{m=1}^{M}\beta^{(m)}(n)\left(\hat{\sigma}^{(m)}(n)\right)^2 \tag{20}$$

$$\left(\hat{\sigma}^{(m)}(n)\right)^2 \quad = \quad \lambda_m\left(\hat{\sigma}^{(m)}(n-1)\right)^2 + (1-\lambda_m)x^{(m)}(n)\ . \tag{21}$$

[4] "Multiple-forgetting-factor tracking" is algorithmically simpler than "adaptive-forgetting-factor adaptation".

[5] This subsection parallels the adoption in [14] of the multiple-forgetting-factor method of [9].

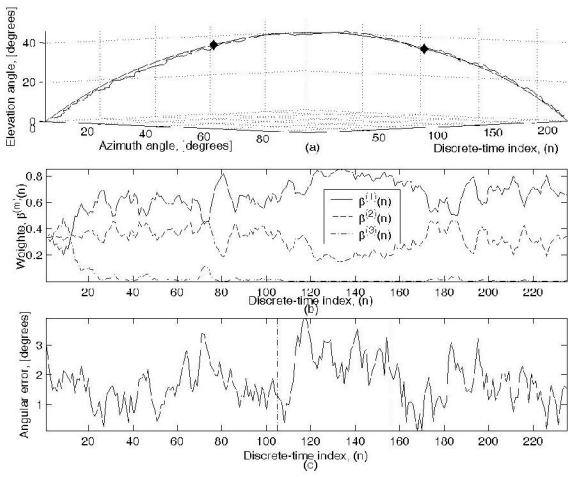

Fig. 1. MFF-RLS tracking of an incident source at "piece-wise constant" angular speed $\gamma(n)$, using a three-element vector-hydrophone (no pressure-hydrophone) placed away from any reflecting boundary.

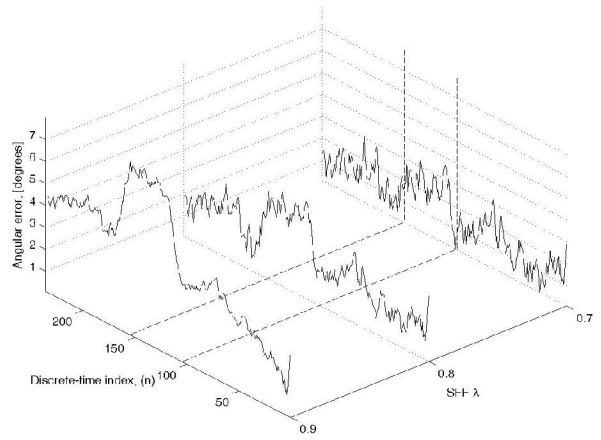

Fig. 2. The angular error $\psi(n)$ for SFF-RLS tracking (at various forgetting-factor values λ) of an incident source at "piece-wise constant" angular speed $\gamma(n)$, using a three-element vector-hydrophone (no pressure-hydrophone) placed away from any reflecting boundary.

In (17), W denotes the integer part of the median of $\left\{\frac{1}{1-\lambda_m},\, m=1,\ldots,M\right\}$.

III. Simulations

Monte Carlo simulations verify the efficacy of the proposed multiple-forgetting-factor (MFF) RLS algorithm using a single vector-hydrophone located at the coordinates' origin, with no prior knowledge of the source's spatial motion or the signal-to-noise ratios $\frac{\sigma_s^2}{\sigma_v^2}$ and $\frac{\sigma_s^2}{\sigma_p^2}$. The unit-power incident source moves along a circular arc with an angular speed of

$$\gamma(n) \;=\; \begin{cases} 0.005, & n\in[0,209] \\ 0.025, & n\in[210,251] \\ 0.01, & n\in[252,357] \end{cases} \qquad (22)$$

radians per discrete-time sample. At discrete-time nT, the source's Cartesian location is $\left[\frac{1}{\sqrt{2}}+\frac{1}{\sqrt{2}}\cos(\gamma(n)),\, \frac{1}{\sqrt{2}}-\frac{1}{\sqrt{2}}\cos(\gamma(n)), \sin(\gamma(n))\right]^T$. Fig. 1-(a)'s solid curve plots the above source movement (θ_n, φ_n) over the discrete time nT.. The solid curve's two diamond icons mark the n-boundaries where $\gamma(n)$ of (22) changes value according to (22).

Fig. 1-(a)'s zigzag curve plots a no-boundary case's tracking estimates $(\hat{\theta}_N, \hat{\varphi}_N)$, obtained from the MFF-RLS algorithm at $M=3, \lambda_1=0.7, \lambda_2=0.8, \lambda_3=0.9$, $\{\beta^{(m)}(n)=\frac{1}{3}, \forall m$ and $n=2-W,\ldots,0\}$. Fig. 1-(b) shows how the three forgetting-factors $\lambda_1,\lambda_2,\lambda_3$ are relatively weighted as $\gamma(n)$ changes over discrete-time n. Fig. 1-(c) plots the corresponding angular error, defined here as the angle between the incident source's true Cartesian coordinates and the algorithm's estimated coordinates: $\psi(n) = \cos^{-1}\left(\frac{(\boldsymbol{a}(nT))^H \hat{\mathbf{d}}(nT)}{\|\boldsymbol{a}(nT)\|\ \|\hat{\mathbf{d}}(nT)\|}\right)$. These subfigures in Fig. 1 show the 3FF-RLS algorithm to closely track the source's azimuth and elevation angles.

To illustrate the MFF-RLS tracking algorithm's superiority over the SFF-RLS algorithm, Fig. 2 and Table III show how the SFF-RLS' tracking error critically depends on the pre-set λ, which equals $0.7, 0.8$, or 0.9 in Fig. 2, with all other simulation settings identical to those of Fig. 1. Fig. 2 is the counterpart of Fig. 1-(c). Table III compares the tracking angular error of 3FF-RLS versus various λ-settings in SFF-RLS. While SFF-RLS at $\lambda=0.8$ gives a time-averaged angular error 2% under 3FF-RLS's, SFF-RLS at $\lambda=0.7$ and $\lambda=0.7$ would give a time-averaged angular error respectively at 13% and 16% over 3FF-RLS's. As $\sigma_s, \sigma_v, \sigma_p$, are typically unknown in practical applications, SFF-RLS could be pre-set at a suboptimal λ value to give significantly higher tracking errors than would MFF-RLS.

Fig. 3 is the counterpart of Fig. 1, now for the near-boundary case at $R(\theta)=1$, $D=\frac{\lambda}{2}$, and ,

$$\gamma(nT) \;=\; \begin{cases} 0.01, & n\in[0,104] \\ 0.021, & n\in[105,155] \\ 0.013, & n\in[156,236] \end{cases} \qquad (23)$$

Fig. 3 verifies the efficacy of the tracking equations (4) to (8). Referring to Table III's bottom half, 3FF-RLS costs a 1% degradation in the time-averaged angular error (relative to the SFF-RLS pre-set at $\lambda=0.8$); however, 3FF-RLS could potentially reduce the time-averaged angular error by up to 12% (relative to the SFF-RLS pre-set at $\lambda=0.9$).

References

[1] C. B. Leslie, J. M. Kendall & J. L. Jones, "Hydrophone for Measuring Particle Velocity," *Journal of Acoustical Society of America*, vol. 28, no. 4, pp. 711-715, July 1956.

[2] G. L. D'Spain, W. S. Hodgkiss & G. L. Edmonds, "The Simultaneous Measurement of Infrasonic Acoustic Particle Velocity and Acoustic Pressure in the Ocean by Freely Drifting Swallow Floats," *IEEE Journal of Oceanic Engineering*, vol. 16, no. 1, pp. 195-207, April 1991.

[3] G. L. D'Spain, W. S. Hodgkiss, G. L. Edmonds, J. C. Nickles, F. H. Fisher & R. A. Harriss, "Initial Analysis Of The Data From The Vertical DIFAR Array," *IEEE Oceans Conference*, vol. 1, pp. 346-351, 1992.

[4] G. C. Chen, & W. S. Hodgkiss, "VLF Source Localization with a Freely Drifting Acoustic Sensor Array," *IEEE Journal of Oceanic Engineering*, vol. 18, no. 3, pp. 209-223, July 1993.

TABLE I

3FF-RLS VERSUS SFF-RLS IN TERMS OF $\bar{\psi}$, THE ALGEBRAIC AVERAGE OF $\{\psi(n), \forall n\}$

	Algorithm	λ_1	λ_2	λ_3	$\bar{\delta}_\psi$
no-boundary	MFF	0.7	0.8	0.9	3.0122
no-boundary	SFF	0.7	-	-	3.4173
no-boundary	SFF	0.8	-	-	2.9522
no-boundary	SFF	0.9	-	-	3.5091
near-boundary	MFF	0.7	0.8	0.9	3.0121
near-boundary	SFF	0.7	-	-	3.3155
near-boundary	SFF	0.8	-	-	3.0444
near-boundary	SFF	0.9	-	-	3.3882

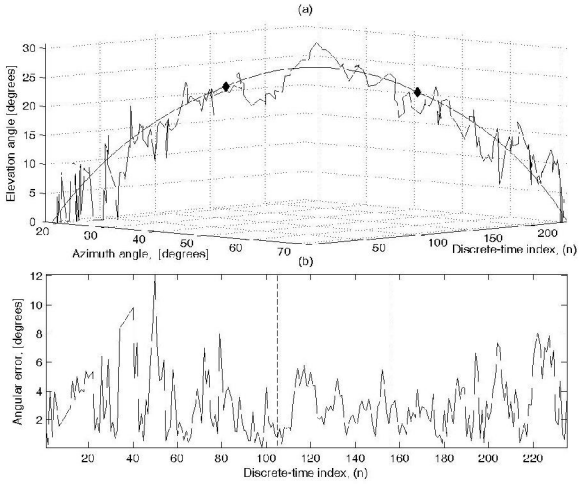

Fig. 3. MFF-RLS tracking of an incident source at "piece-wise constant" angular speed $\gamma(n)$, using a three-element vector-hydrophone (no z-axis velocity-hydrophone) placed half-wavelength from a rigid reflecting boundary.

[5] V. A. Shchurov, V. I. Ilyichev and V. P. Kuleshov, "Ambient Noise Energy Motion in the Near Surface Layer in Ocean Wave-Guide," *Journal de Physique*, vol. 4, no. 5, part 2, pp. 1273-1276, May 1994.

[6] A. Nehorai & E. Paldi, "Acoustic Vector-Sensor Array Processing," *IEEE Transactions on Signal Processing*, vol. 42, no. 10, pp. 2481-2491, September 1994.

[7] M. J. Berliner & J. F. Lindberg, *Acoustical particle velocity Sensors: Design, Performance and Applications*, Woodbury, New York, U.S.A.: AIP Press, 1996.

[8] B. Hochwald & A. Nehorai, "Identifiability in Array Processing Models with Vector-Sensor Applications," *IEEE Transactions on Signal Processing*, vol. 44, no. 1, pp. 83-95, January 1996.

[9] K. Uosaki, M. Yotsua & T. Hatanaka, "Adaptive Identification of Nonstationary Systems with Multiple Forgetting Factors," *IEEE Conference on Decision & Control*, vol. 1, pp. 851-856, 1996.

[10] K. T. Wong & M. D. Zoltowski, "Closed-form Underwater Acoustic Direction-Finding with Arbitrarily Spaced Vector-Hydrophones at Unknown Locations," *IEEE Journal of Oceanic Engineering*, vol. 22, no. 3, pp. 566-575, July 1997.

[11] K. T. Wong & M. D. Zoltowski, "Extended-Aperture Underwater Acoustic Multisource Azimuth/Elevation Direction-Finding Using Uniformly But Sparsely Spaced Vector Hydrophones," *IEEE Journal of Oceanic Engineering*, vol. 22, no. 4, pp. 659-672, October 1997.

[12] M. Hawkes & A. Nehorai, "Acoustic Vector-Sensor Beamforming and Capon Direction Estimation," *IEEE Transactions on Signal Processing*, vol. 46, no. 9, pp. 2291-2304, September 1998.

[13] V. A. Shchurov & M. V. Kuyanova, "Use of Acoustic Intensity measurements in Underwater Acoustics (Modern State and Prospects)," *Chinese Journal of Acoustics*, vol. 18, no. 4, pp. 315-326, 1999.

[14] A. Nehorai & P. Tichavsky, "Cross-Product Algorithms for Source Tracking Using an EM Vector Sensor," *IEEE Transactions on Signal Processing*, vol. 47, no. 10, pp. 2863-2867, October 1999.

[15] K. T. Wong & M. D. Zoltowski, "Root-MUSIC-Based Azimuth-Elevation Angle-of-Arrival Estimation with Uniformly Spaced but Arbitrarily Oriented Velocity Hydrophones," *IEEE Transactions on Signal Processing*, vol. 47, no. 12, pp. 3250-3260, December 1999.

[16] K. T. Wong, "Adaptive Source Localization & Blind Beamforming for Underwater Acoustic Wideband Fast Frequency-Hop Signals of Unknown Hop Sequences & Unknown Arrival Angles Using a Vector-Hydrophone," *IEEE Wireless Communications & Networking Conference*, vol. 2, pp. 664-668, 1999.

[17] K. T. Wong & M. D. Zoltowski, "Self-Initiating MUSIC-Based Direction Finding in Underwater Acoustic Particle Velocity-Field Beamspace," *IEEE Journal of Oceanic Engineering*, vol. 25, no. 2, pp. 262-273, April 2000.

[18] M. Hawkes & A. Nehorai, "Acoustic Vector-Sensor Processing in the Presence of a Reflecting Boundary," *IEEE Transactions on Signal Processing* vol. 48, no. 11, pp. 2981-2993, November 2000.

[19] J. Hui, H. Liu, M. Fan & G. Liang, "Study on the Physical Basis of Pressure and Particle Velocity Combine Processing," *Chinese Journal of Acoustics*, vol. 20, no. 3, pp. 203-212, 2001.

[20] X. Liu, J. Xiang & Y. Zhou, "Passive Tracking and Size Estimation of Volume Target Based on Acoustic Vector Intensity," *Chinese Journal of Acoustics*, vol. 20, no. 3, pp. 225-238, 2001.

[21] P. Tichavsky, K. T. Wong & M. D. Zoltowski, "Near-Field/Far-Field Azimuth and Elevation Angle Estimation Using a Single Vector Hydrophone," *IEEE Transactions on Signal Processing*, vol. 49, no. 11, pp. 2498-2510, November 2001.

[22] K. T. Wong & H. Chi, "Beam Patterns of an Underwater Acoustic Vector Hydrophone Located Away from any Reflecting Boundary," *IEEE Journal of Oceanic Engineering*, vol. 27, no. 3, pp. 628-637, July 2002.

[23] J. A. McConnell, "Analysis of a Compliantly Suspended Acoustic Velocity Sensor," *Journal of Acoustical Society of America*, vol. 113, no. 3, pp. 1395-1405, March 2003.

[24] M. Hawkes & A. Nehorai, "Wideband Source localization Using a Distributed Acoustic Vector-Sensor Array," *IEEE Transactions on Signal Processing* vol. 51, no. 6, pp. 1479-1491, June 2003.

[25] Q. Lu, S. Yang, J. Zhang, S. Piao, "High Resolution DOA Estimation in Beam Space Based on Acoustic Vector-Sensor Array," *Journal of Harbin Engineering University*, vol. 25, no. 4, pp. 440-445, August 2004.

[26] H.-W. Chen & J. Zhao, "Coherent Signal-Subspace Processing if Acoustic Vector Sensor Array for DOA Estimation of Wideband Sources," *Signal Processing*, vol. 85, pp. 837-847, April 2005.